HHS Public Access

Author manuscript

Carbohydr Polym. Author manuscript; available in PMC 2018 December 01.

Published in final edited form as:

Carbohydr Polym. 2017 December 01; 177: 49–57. doi:10.1016/j.carbpol.2017.08.058.

Hydroxypropyl Methylcellulose-based Controlled Release Dosage by Melt Extrusion and 3D Printing: Structure and Drug Release Correlation

Jiaxiang Zhang[1], **Weiwei Yang**[2], **Anh Q. Vo**[1], **Xin Feng**[1], **Xingyou Ye**[1], **Dong Wuk Kim**[1], and **Michael A. Repka**[1,3,*]

[1]Department of Pharmaceutics & Drug Delivery, The University of Mississippi, University, MS 38677, USA

[2]Department of Chemistry and Biochemistry, The University of Mississippi, University, MS 38677, USA

[3]Pii Center for Pharmaceutical Technology, The University of Mississippi, University, MS 38677, USA

Abstract

The objective of this study was to develop a new approach for fabrication of zero order release of active pharmaceutical ingredients (APIs) using hot-melt extrusion (HME) and 3D printing technology to generate tablets with specific 3D structures. By correlating the geometry of the 3D printed tablets with their dissolution and drug release rates, mathematical models that have been developed to describe drug release mechanisms were also studied. Acetaminophen was used as a model drug, and Benecel™ hydroxypropyl methylcellulose (HPMC) E5 and Soluplus® were used to formulate nine fuse depositional 3D-printed tablets with different inner core fill densities and outside shell thicknesses. This work reports the successful fabrication of solid-dispersion filaments with an API dispersed in HPMC based matrix via HME technology, and the production of zero order controlled release tablets with different 3D structures (tablets #3, 5, 6, and 9) using a 3D printer.

Graphical Abstract

*Address for correspondence: Michael A. Repka, D.D.S., Ph.D. Professor and Chair, Department of Pharmaceutics and Drug Delivery, Director, Pii Center for Pharmaceutical Technology, School of Pharmacy, The University of Mississippi, University, MS 38677, Phone: 662-915-1155, Fax: 662-915-1177, marepka@olemiss.edu.

Disclosure: The authors report no conflicts of interest in this work.

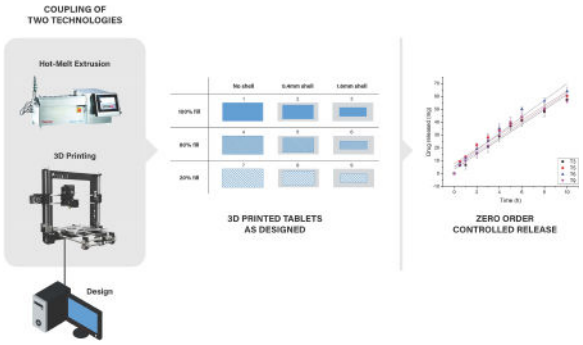

Keywords

Hydroxypropyl methylcellulose; Acetaminophen; Hot-melt extrusion; Fused deposition modeling 3D printing; Controlled release; Dissolution kinetics

1. Introduction

Drug delivery systems (DDSs) are methods of administering active pharmaceutical ingredients (APIs) to achieve a therapeutic effect in humans or animals. They aim to ensure optimal drug distribution and absorption and improve efficacy and safety by controlling the rate, time, and target of drug release in the body (Jain, 2008). Approaches for effective DDSs include controlled release formulations, in which the drug is released at a controlled rate over a set period of time and targeted delivery (Santos et al., 2011; Weiniger et al., 2012), in which the drug is only active in a targeted area of the body, such as in cancerous tissues (Shimoni et al., 2012; Ward et al., 2013). Controlled release technologies can be broadly categorized into liposomal (Willis, Hayes, & Mansour, 2012), electromechanical (Staples et al., 2006), and polymeric types (Vo et al., 2016). The use of liposomes for controlled delivery has been widely studied, but *in vivo* instability and entrapment by the reticuloendothelial system are two major obstacles to be overcome (Paavola et al., 2000). The use of pumping devices to control the amount of drug released is in principle the most direct and sophisticated approach; however, osmotic pump systems are much more expensive and may be subject to dose dumping if the membrane breaks (Santus and Baker, 1995). Polymeric controlled release systems, which use biodegradable, non-biodegradable, and soluble polymers as drug carriers, can be administered via parenteral, implantation, oral, insert, and transdermal routes (Leong & Langer, 1988). Nowadays, polymeric oral-controlled release technologies are considered economical and immediately applicable in drug development, improving patients' quality of life by reducing the inconvenience caused by the frequent dosing of conventional tablets (Kojima et al., 2008). Furthermore, the increased use of additive manufacturing, also known as 3D printing technology, provides an effective solution for individual, complex production of oral-controlled DDSs (Abbadessa et al., 2016). 3D printing is the layer-by-layer production of 3D objects from digital designs (Gross et al., 2014). Compared with developing new materials for drug delivery, the development of new material fabrication tools and protocols is more efficient and economical. 3D printing technology provides an alternative means of engineering release

profiles, by controlling the spatial distribution within a given polymer composition rather than creating a new host material (Moulton & Wallace, 2014).

Hot-melt extrusion (HME) is a manufacturing technique that, unlike traditional oral dosage manufacturing techniques, such as direct compression and tableting (Sarode et al., 2013),generally involves the use of twin-rotor extruders that process water-soluble polymeric excipients, mixing them with APIs while molten to cause partial or total API dissolution, and pump the homogeneous mixture through a die to form an extrudate containing the API in a stable form (Stanković, Frijlink, & Hinrichs, 2015).

HME has been used in the plastic and rubber industries since the 1930s. Pharmaceutical HME is currently being investigated by both industry and academia as a means to increase the release rate of poorly water-soluble APIs by melt-mixing them with hydrophilic, water-soluble polymers (Repka, Langley, & DiNunzio, 2013). HME can help overcome poor API bioavailability, create new modified-release drug systems, and mask bitter tastes (Sarode, Malekar, Cote, & Worthen, 2014). At the same time, an increasing body of literature exists on the production of controlled release dosages by melt-mixing readily water-soluble APIs with rate-controlling polymers.(Sarode, Obara, et al., 2014)

Compared to traditional pharmaceutical manufacturing processes, combining HME and 3D print technology as a continuous process highlights their respective advantages to 1) increase the solubility and bioavailability of poorly water-soluble drugs; and 2) produce more complex structured dosages and personalized drug products. In addition, combining the technologies reduces the required downstream processing, making it more efficient and economical. The Food and Drug Administration (FDA) has recently encouraged the production of oral solid dosages that meet the increasing demands of oral drug delivery in terms of API bioavailability and drug release characteristics, in a continuous and controlled process (O'Connor, Lawrence, & Lee, 2016).

The basic steps involved in continuous pharmaceutical HME/3D printing dosage production are 1) dosage design and conversion to a printer-readable format; 2) raw material preparation (powders, particulates, granules, pastes, etc.); 3) HME to produce filaments; 4) filament cooling; 5) 3D printing; and 6) removal and downstream processing (such as cooling, drying, and packing, etc.) In continuous pharmaceutical HME/3D printing, extrusion of the 3D printable filaments is a very important step, along with dissolving poorly water-soluble APIs into molten polymeric excipient and mixing, which improves the final dosage bioavailability (Zhang et al., 2016).

The aim of this novel study was to couple fused deposition modeling (FDM) 3D printing with HME technology to print hydroxypropyl methylcellulose (HPMC)-based controlled release tablets with various structural designs and drug release profiles.

2. Material and methods

2.1. Materials

Acetaminophen (APAP; Spectrum Chemical, New Brunswick, NJ, USA) was selected as a model API. APAP is crystalline, and in the Biopharmaceutics Classification System is considered a borderline compound between class I (high permeability, high solubility) and class III (low permeability, high solubility), with a melting point of 169–170°C (Kalantzi et al., 2006). Benecel™ HPMC E5 was donated by Ashland Inc. (Covington, KY, USA). HPMC has been investigated for the preparation of oral drug delivery systems and is one of the most widely used hydrophilic matrix materials (Banks et al., 2014; Colombo, 1993). It can significantly affect the release kinetics of APAP due to its high swellability (Siepmann and Peppas, 2012). Once the tablets contact the dissolution media, the polymer chain will have relaxed with volume expansion, thus it diffuses into the matrix (Brannon-Peppas and Peppas, 1991), then, the APAP diffuses out of the system (Pani & Nath, 2014). HPMC E5 has an average molecular weight of 34,500 Da and normal viscosity of 4.0–6.0 mPa·S.Soluplus® was donated by BASF (Ludwigshafen, Germany) and is a co-polymer of polyethylene glycol, polyvinyl acetate, and polyvinylcaprolactam-based graft with an amphiphilic chemical structure, particularly developed for solid dispersions, which acts as a polymeric solubilizer. Due to its functional groups, it can both solubilize poorly water-soluble APIs in aqueous media and act as a matrix polymer in solid dispersions (Djuris et al., 2013). All other reagents were either HPLC- or analytical-grade.

2.2. Methods

2.2.1. Formulation—APAP, Soluplus®, and HPMC E5were combined at a weight ratio of 1:2:7 and tumble-mixed on a Maxiblend™ (GlobePharma, New Brunswick, NJ, USA) at 25 rpm for 30 min, after filtration through a US#30 mesh screen to remove any aggregates that may have formed.

2.2.2. HME—The extruder used in this study was a co-rotating, twin screw extruder with 11 mm diameter screws, a length/diameter ratio of 40, and eight electrically-heated zones (Thermo Fisher Scientific, Waltham, MA, USA); feeding zone temperature was controlled by an external circulation heater. Physical mixtures were extruded at 160°C for all zones with a standard screw configuration at a screw speed of 50 rpm. A 2 mm-round die was used to extrude filaments for the 3D printer. A conveyor belt was used to cool and straighten the filaments for feeding into the 3D printer.

2.2.3. Differential scanning calorimetry (DSC)—A Diamond DSC system (PerkinElmer, Waltham, MA, US) was used to study drug crystallinity and characterize drug miscibility in the extrudates. Samples (2–5 mg) were hermetically sealed in an aluminum pan and heated from 40–200°C at a rate of 10°C/min. Ultra-purified nitrogen was used as the purge gas at a flow rate of 50 mL/min in all DSC experiments. Data were collected and analyzed with Pyris software (PerkinElmer).

2.2.4. Thermogravimetric analysis (TGA)—During HME processing, a PerkinElmer Pyris 1 TGA calorimeter was used to determine the thermal stability of APAP and the

polymers. The samples were placed in an open aluminum pan and heated from 30–300°C at a rate of 20°C/min. Ultra-purified nitrogen was used as the purge gas at a flow rate of 25 mL/min. Data were collected and analyzed using Pyris software, and percentage mass loss and/or onset temperatures were calculated.

2.2.5. 3D printing—The model tablets were designed using Microsoft 3D Builder (Microsoft, Redmond, WA, USA), sliced using CURA software (version 15.04; Ultimaker, Geldermalsen, The Netherlands), and then converted to .gcode files. Nine tablets were designed, with the same overall tablet dimensions (diameter, 10 mm; thickness, 4.5 mm), but with different outside shell thicknesses or core fill densities (Figure 1). Tablets were fabricated from the extruded filaments using a commercial FDM-3D printer (Prusa i3 3D desktop printer, Prusa Research, Prague, Czech Republic) with an extruder, which had an E3D v6 HotEnd and a 0.4 mm nozzle. The best tablets were produced using standard resolution with the raft option activated, and an extrusion temperature of 200°C. Other settings used were as follows: bed temperature, 50°C; printing speed, 50 mm/s; nozzle traveling speed, 50 mm/s; layer height, 0.10 mm. The dimensions and weights of the 3D printed (3DP) tablets were then measured. To determine the dissolution kinetics, empty tablets (1.6 mm and 0.4 mm outside shell) were also printed.

2.2.6. Assessment of tablet morphology—A digital caliper (VWR®, PA, USA) was used to determine the diameters and thicknesses of the tablets, and cross-sectional images of the 3DP tablets were acquired using a JOEL JSM 5610LV scanning electron microscopy (SEM) (JOEL, MA, USA).(Feng et al., 2016)

2.2.7. Determination of tablet strength—A standard tablet hardness tester (VK200; Agilent Technologies, Santa Clara, CA, USA) with a maximum force of 35 kp was used to measure tablet hardness. Six tablets from each group were tested.

2.2.8. *In vitro* drug release—Drug release from different 3D structured tablets was determined using a United States Pharmacopeia (USP) dissolution apparatus II (Hanson SR8-plus™; Hanson Research, Chatsworth, CA, USA). Dissolution tests were conducted as per US Pharmacopeia standards using Simulated Intestinal Fluid^{TS} (without pancreatin, pH 6.8), which is representative of the small intestinal fluid of humans. Each experiment was carried out in triplicate using 900 mL of dissolution medium at 37 ± 0.5°C for 24 h. The paddle speed was set at 50 rpm. Due to their porous internal structures, tablets #8 and 9 floated; therefore, sinkers were used to keep the tablets submerged in the dissolution vessel. Samples were analyzed at 0.5, 1, 2, 4, 5, 6, 8, 10, 12, and 24 h. The amount of released APAP was determined by HPLC (Waters Corp., Milford, MA, USA) at 246 nm and analyzed using Empower software (version 2, Waters Corp.).

2.2.9 Dissolution kinetic studies—One of the main objective is combining the HME and 3D print to produce the zero order released dosages by optimizing the 3D structure. In order to investigate the dissolution kinetics, dissolution data were fitted to several mathematic models including Higuchi model, Ritger-Peppes model, Peppes-Sahlin model, and zero order model, a correlation coefficient (R^2) was used to evaluate the accuracy of an individual model.

3. Results and discussion

3.1. Preliminary study of raw materials

TGA can provide information about decomposition or drug degradation (Coats & Redfern, 1963). According to the TGA results, mass loss of APAP and the physical mixtures emerged at temperatures above 350°C, indicating that the drug and polymer matrix would not degrade during melting extrusion at 160°C and 3D printing at 200°C. Extruded filaments were fed into the 3D printer HotEnd by feeding gears at 14 °C, and then melted in the HotEnd hose, avoiding drug decomposition or degradation during the printing process. Though a standard screw configuration with 3 different mixing zones was utilized during HME processing, which would have a high shear force resulting in drug decomposition or degradation, drug content result was confirmed with final in vitro drug release studies.

DSC is a thermoanalytical technique to detect phase transitions in samples, with the premise that when the sample undergoes a phase transition, more heat will be required than that required by a reference sample.(Feng et al., 2015) The APAP DSC curve exhibited a peak at 172°C. A heat-cool-heat method was utilized for DSC analysis of the physical mixture. As expected, the physical mixture showed an obvious peak at approximately 170°C during the first heating process and no peak during the second heating process. This result indicated that APAP can disperse or dissolve into the molten polymer matrix during HME processing, forming an amorphous solid dispersion.

3.2. Tablet morphology study

3.2.1. 3D structure—All tablets were successfully printed with designed 3D structures. Due to space limitations, one sample (tablet #5, with a 0.4 mm shell and 80% inner fill) is shown in Figure 2. Tablets were broken and split apart rather than cut, as the blade would destroy the inner 3D structures. Figure 2a shows the clearly layered structure of the 0.4 mm shell and inner fill. Figure 2b shows a cross section of porous structure of the inner fill. Figure 2c demonstrates the layered structure of the tablet shell.

As shown in Figure 3a, in tablets without an outside shell, the porous inner fill structure is in direct contact with the medium, while in the 0.4 mm and 1.6 mm shell tablets, the outside shell acts as a barrier for the inner porous structure, preventing the core from direct contact with the medium. Due to the erosion and swelling effects of HPMC and Soluplus®, the tablets slowly dissolve in dissolution medium rather than disintegrate(Liu et al., 2012); therefore, tablets with 16 mm shell thickness should dissolve not only much slower but also at more constant rates than the other tablets

As shown in figure 3b, tablets with 100% core fill density have a very solid structure with limited surface area, and were expected to have the slowest drug release rates. Tablets with 80% and 20% fill density exhibited porous structures with larger surface areas. However, low inner fill density will also affect the hardness of the tablets.

3.2.2. Tablet morphology—Images from the tablet morphology study and SEM analyses revealed that the 3DP tablets had smooth surfaces and a tight structure. Generally, tablets with a higher core fill density or thicker shells had higher density and hardness than tablets

with lower core fill and thinner shells (Table 1). The hardness of tablets designed with 100% fill exceeded the detection limit of the hardness tester, and tablets with 80% fill were harder than tablets with 20% fill. The outside shell thickness also affected hardness, as tablet #9, with a 1.6 mm shell,was much harder than other tablets with same fill density. The hardness test can only measure stress towards the tablets; however, in the vertical direction, the structure was loose and easy to split, even when the hardness exceeded the limit of detection.

The volume of each cylindrical tablet was calculated as follows:

$$V=\frac{\pi D^2}{4}*h \quad \text{Eq 1}$$

Where D and h are the diameter and thickness of the tablets, respectively. Thus, the theoretical density of a tablet was calculated according to the following equation:

$$\rho=\frac{m}{V}=\frac{4m}{\pi D^2*h} \quad \text{Eq 2}$$

where m is the weight of the tablet. The density of the HME-generated filaments was calculated using the same equation. As shown in Table 1 the theoretical density of 3DP tablets was much higher than that of unprinted filaments. In addition, tablets with high hardness and density values are expected to have delayed dissolution and slow drug release after administration. In the geometric study, the tablets had only small variations in weight (the largest is T7, at ~7%) and dimensions, which demonstrate the good reproducibility of the 3D printing process. Based on the weight of the tablets and shell without inner fill, the 0.4 mm shell was approximately 47.99% of the overall weight of T2, 53.04% of T5, and 79.31% of T8. The weight of the 1.6 mm shell was approximately 80.09% of the overall weight of T3, 82.42% of T6, and 96.77% of T9.

3.2.3. Porosity study of the tablets—The discussion of the porosity of the tablets was added and highlighted in the section 3.2.3.

From the observation of the SEM pictures (figure not shown), the extrudate filament was robust and shown no porous structure, as well as the materials extruded from the nozzle of the printer, so the porosity all comes from the tablet 3D structure design. The porosity of the 3D printed tablets can be expressed using the following equation (Vo et al., 2017):

$$P=\frac{V_{\text{void}}}{V_{\text{geometric}}} \quad \text{Eq 3}$$

where the V_{void} is the total volume of the empty space inside the tablets, and the $V_{geometric}$ is the volume of the tablets as a whole object. As shown in figure 3, 100% filled tablets can be

considered as solid and no porous structure, and the porosity of tablets #4 and #7 can be considered as the designed fill density. Based on the geometry measurement and tablets design, the calculated porosity of the tablets was listed in the table 1. Tablet #7 and #8 shows fast release rates than the other tablets with same shell because both the thin shell and porous structure. For the other tablets, due to the robust shell structure and swelling of the matrix, the inner core porous structure has limited impact on the dissolution kinetics.

3.3.*In vitro* drug release

3.3.1. Drug release profiles—As shown in Figure 4, tablets with 1.6 mm shells had extended drug release rates due to the 3D structure of the thicker shell, while tablets without shells exhibited fast release profiles, because the inner structures were loose and direct contact with the dissolution media. The 0.4 mm shell was totally dissolved within 4 h, which was confirmed by drug release studies, showing 100% drug release in 4 h. Based on the tablet geometry study, the calculated weight ratios of 0.4 mm shells were 47.99%, 53.04%, and 79.31% for T2, T5, and T8, respectively, and the percentage of drug released after 4 h was 52.91%, 54.27%, and 79.41%, respectively, suggesting that the inner core releases the drug after the shell is dissolved.Tablets with 1.6 mm shells released APAP over a longer period, with 71%, 79%, and 66% of drug released after 8 h from T6, T7, and T8, respectively. In the 100% fill tablets, the drug release rate from T1, which had no shell, was higher than those for T2 and T3, which indicated that the inner core with 100% fill has a looser structure than the shell. T7 (20% inner fill, no shell) exhibited74% drug release within 0.5 h and 85% drug release in 1 h, and all tablets without shells had released at least 70% of the drug within 4 h. The linear regression of no shell tablets was lower than 0.88. As expected, the released rate was 100%< 80%< 20%.

The drug dissolution rates of tablets with each designed 3D structure were evaluated. Poorly water-soluble APIs can disperse or dissolve in polymer matrices to form solid dispersions or solutions during the HME process (Serajuddin, 1999). As mentioned in the DSC results, APAP was completely dissolved into the polymer matrix, forming an amorphous solid dispersion. The observed dissolution and drug release rates from the HPMC based matrix were influenced by the 3D geometric structure and composition, and the following phenomena were observed in the *in vitro* drug release study:

1. Once the tablets contacted the dissolution media, a steep concentration gradient formed at the media/tablet interface. Here, water acted as a plasticizer and reduced the glass transition temperature (T_g) of the system. Once the system reached the T_g during the *in vitro* study, the matrix transformed to hydrogel (Siepmann & Peppas, 2012).
2. The HPMC-based matrix swelled and formed hydrogel while the media were penetrating, which changed the drug concentration at the media/tablet interface. Matrix imbibition of the media through the tight shell structure was the most important rate-controlling step during the dissolution study. The media took longer to penetrate through the thicker shell than through the thinner shell and inner core.

3. The concentration gradients led the APAP to diffuse from the media/tablet interface to the hydrogel, and thus into the dissolution media.

4. The more porous lower fill density was less restrictive for drug diffusion upon drug depletion, meaning that APAP dissolved and diffused more rapidly from the HPMC chain. Conversely, due to the tight structure of the high fill density and thicker shell, the APAP was slowly released from the matrix.

All groups of tablets achieved ~100% drug release within 24 h, confirming that no API or excipient degradation occurred during the HME or 3D printing processes. There are various mathematical kinetic models that can be applied to describe *in vitro* drug release kinetics, such as Higuchi (Higuchi, 1961), Ritger-Peppas (Ritger & Peppas, 1987), Sahlin-Peppas (Peppas & Sahlin, 1989), first order, and zero order, which help researchers understand release mechanisms and optimize formulations. Drug release can be considered either Fickian or non-Fickian diffusion. In Fickian diffusion, the drug release rate is independent of the drug concentration in the matrix (Gillespie & Seitaridou, 2012).

3.3.2. Dissolution kinetic studies—Higuchi equation is developed by Higuchi in 1961, which is one of the most famous and most often used mathematical model to describe the drug release rate from the matrix systems (Bunge, 1998).The original equation of Higuchi model is:

$$\frac{M_t}{A} = \sqrt{D(2 * C_0 - C_s) * C_s * t} \quad \text{Eq 4}$$

here M_t is the accumulative drug released in time t; A is the overall contact surface of the matrix to the medium; D is the drug diffusivity in the polymer; C_0 and C_s are the drug concertation at beginning time and solubility in the polymer. Such equation can be simplified as following:

$$\frac{M_t}{M_\infty} = k_H * t^{1/2} \quad \text{Eq 5}$$

where the cumulative amount of the drug in the system, k_H is a constant contains the information of the structure and geometry of the matrix (Peppas & Narasimhan, 2014). The Higuchi model initially only applicable for planer systems and then was modified and extended by researchers for variety of matrix (Higuchi, 1963; Paul, 2011; Siepmann and Siepmann 2012). The accumulative released drug is proportional to the square root of time. Researchers point out the original equation can only be used for “ideal” controlled released matrix because it was derived under pseudo-steady states and it validity is dependent upon the following assumptions (Siepmann & Göpferich, 2001):

i. The initial drug concentration is much higher than the drug solubility.

ii. Drug diffusion is one-dimensional, making edge effects negligible.

iii. The suspended drug micro- or nanoparticles are much smaller than the thickness of the system.

iv. Swelling or dissolution of the polymer carrier can be neglected.

v. The drug diffusion coefficient is constant.

vi. Perfect sink conditions prevail and are maintained.

Higuchi model was not applicable for this work because the 3D printed matrix may diffusion multidimensional and the swelling of the matrix is unneglectable, the initial drug concentration of *in vitro* study can't meet the assumptions listed above as well.

We applied the data from the *in vitro* drug release study to the Ritger-Peppas model (also as known as “power law”), a simple model that exponentially relates the drug release to the fractional release of the drug, developed by Peppas et al. in 1983. The Ritger-Peppas model can be described as the following:

$$\frac{M_t}{M_\infty} = k * t^n \quad \text{Eq 6}$$

where M_t is the cumulative amount of drug released at time t, M_∞ is the total amount of drug, k is a constant incorporating structural and geometric characteristics of the device, t is the time at which drug release is calculated or measured, and n is the release exponent, indicative of the mechanism of drug release (Korsmeyer, Gurny, Doelker, Buri, & Peppas, 1983).

Ritger and Peppas's work shows this model has good ability for fitting before reaching approximately 60% total amount of drug release, and the equation has two distinct physical realistic meanings in the special cases of 0.45 (Fickian diffusion) and 0.89 (Case II transport). The Case II transport mechanism is a very near approximation of a normal Fickian diffusion process. If 0.45< n< 0.89, it indicates the superposition of both phenomena (anomalous transport). These two extreme values for the exponent n are only valid for cylinder geometry (Ritger and Peppas, 1987).

All the calculated data are listed in Table 2. Though the shape were cylindrical, the tablets has different density along the axial direction from the core due to the specific 3D structure design, and T3 (n=0.78, R^2=09808), T6 (n=0.82, R^2=0.9968), and T9 (n=0.79, R^2=0.9900) can be considered Case II transport, which can be defined to approximate Fickian diffusion. The drug release rate from HPMC-based matrix with a shell design can be dominated by the swelling kinetics of the polymer, resulting in Case II transport. For T2, n=0.10, indicating Fickian diffusion, but the tablet dissolved too quickly, with 74% of drug released by the first sample collection point at 0.5 h, and R^2=0.8971 indicates that there was limited accuracy when applying the model to T2. For other tablets, the exponent n varied from 0.59–0.71, indicating that both the swelling and diffusion kinetics controlled the drug release rate from the matrix. Peppas and Sahlin also developed a model to analyze anomalous transportation:

$$\frac{M_t}{M_\infty}=k_1 * t^m+k_2 * t^{2m} \quad \text{Eq 7}$$

where k_1, k_2, and m are constants. The first term on the right-hand side represents the Fickian diffusional contribution, whereas the second term the Case II swelling contribution. The coefficient m is the purely Fickian diffusion exponent which has same meaning with the n in Ritger-Peppas model. The percentage of drug released due to the Fickian mechanism, F, is calculated as:

$$F=\frac{1}{1+\frac{k_2}{k_1}t^m} \quad \text{Eq 8}$$

The ratio of both contributions can be calculated as follows:

$$\frac{R}{F}=\frac{k_2 * t^m}{k_1} \quad \text{Eq 9}$$

Such equations were applied to investigate the effect of the differently designed 3D structures on drug release; however, significant effects on the resulting R/F-ratios were found with the investigated 9 different tablets and shells (Table 2). Here the Fickian contribution can be expressed as a function of t^m, then the relaxational contribution can be expressed as a function of t^{2m}. Compared with the n in equation 5 and m in equation 6, $m \neq n$, thus the relaxational mechanism is not negligible (Peppas and Sahlin, 1989). For tablets T1 and T2, though the R^2 values were good, the k_2 was negative when applying the Peppas-Sahlin model, making the data nonsensical and indicating that the drug releasing mechanism were anomalous transport. For tablets T7 and T8, the drug release reached 60% in 2 h, which lacking data for calculating the k_1, k_2, and m. It is difficult to determine the importance of the Fickian or Case II mechanisms without using equations 7 and 8. Figure 5 shows that along with the time or the drug released from the matrix, the Fickian diffusion domination decrease for the first 6 h or 60% of drug released from tablet T5, and the tablet T3 R/F curve indicating that the drug release was dominated by the swelling mechanism. Tablets T4, T6, and T9 were predominated by Fickian diffusion then the swelling mechanism. In this study, the domination of the diffusion mechanism was decrease along with the time or the dissolution of the matrix. Both the diffusion and swelling mechanism indicating the constant and steady drug release rate. Summarize the result of Ritger-Peppas and Peppas-Sahlin model, tablets T3, T5, T6, and T9 can be a proper candidate for zero order drug release.

3.3.3. Zero order drug release—Zero order release, in which the drug release rate is constant over a period of time, is the ultimate goal of all controlled release DDSs. The equation for zero-order release is as follows:

$$M_t = M_0 + k * t \quad \text{Eq 10}$$

where $\boldsymbol{M_t}$ is the cumulative amount of drug released at time t, $\boldsymbol{M_0}$ is the initial amount of drug, $\boldsymbol{K}$ is the release kinetic constant, and $\boldsymbol{t}$ is the time at which the drug release is calculated or measured. As all the tablets reached 80% drug release within 10 h, linear fitting of *in vitro* drug release data from all 9 tablet types are listed in Table 2. Due to the tight structure of the shell, the 1.6 mm shell was totally dissolved within 24 h, and the drug release from the 1.6 mm shell (linear regression R^2=0.9950), T3 (linear regression R^2=0.9790), T6 (linear regression R^2=0.9585), and T9 (linear regression R^2=0.9271) was steady and constant (Figure 6), meaning that the tight structure of the shell resulted in nicely controlled (zero order) drug release rates. T4 (linear regression R^2=0.8472) was almost zero order released, however when plot the first 6 h release data, that the T4 (linear regression R^2=0.9966) and can be considered as zero order release, which confirmed the diffusion mechanism and swelling mechanism dominated the T4 contributes to the constant and steady 60% drug release. The linear fitting results were consistent with the fitting of the Ritger-Peppas and Peppas-Sahlin models, in which drug release from T3, T5, T6, and T9 was constant and steady.

4. Conclusions

In this study, we successfully fabricated solid-dispersion filaments with the API dissolved in a polymer matrix via HME technology. Extruded filaments prepared based on HPMC were printed with optimized 3D printing parameters, producing controlled release tablets with different 3D structures. Based on Ritger-Peppas model fitting, drug release from HPMC-based matrix tablets T3, T6, and T9 may be considered Case II transportation diffusion, indicating that the rate of drug release is independent of time and concentration. Based on the Peppas-Sahlin model, T3, T4, T5, T6, and T9 were dominated by either diffusion or swelling mechanisms. T3, T6, and T9 also had constant and steady drug release rates by linear fitting, confirming that the diffusion model can be considered sustained (zero order) release. In other words, compared to changing the formulation, polymer, or further processes, such as coating, 3D structure design is effective and efficient for optimizing controlled drug release rates. In this work, the thick and tight outside shell structure act as a “barrier” during the in vitro drug release study, which contributes to the slow forming hydrogel and constant control of the drug release rate from the HPMC based matrix. Even though the inner fill tablet is 100% (T1), it cannot perform as well as the outside shell tablets (T3, T6, and T9). This study clearly demonstrates that coupling FDM-based 3D printing with HME offers a novel, economical, and efficient method for manufacturing complex, personalized dosage forms and better controlled release profiles dosages that can be prepared as required for individuals.

Acknowledgments

This work was partially supported by Grant Number P20GM104932 from the National Institute of General Medical Sciences (NIGMS), a component of NIH. The authors also thank the Pii Center for Pharmaceutical Technology for contributions in this project.

References

Abbadessa A, Blokzijl MM, Mouser VHM, Marica P, Malda J, Hennink WE, Vermonden T. A thermo-responsive and photo-polymerizable chondroitin sulfate-based hydrogel for 3D printing applications. Carbohydrate Polymers. 2016; 149:163–174. https://doi.org/https://doi.org/10.1016/j.carbpol.2016.04.080. [PubMed: 27261741]

Banks SR, Pygall SR, Bajwa GS, Doughty SW, Timmins P, Melia CD. The influence of substituted phenols on the sol:gel transition of hydroxypropyl methylcellulose (HPMC) aqueous solutions. Carbohydrate Polymers. 2014; 101:1198–1204. https://doi.org/https://doi.org/10.1016/j.carbpol.2013.10.061. [PubMed: 24299892]

Brannon-Peppas L, Peppas NA. Equilibrium swelling behavior of pH-sensitive hydrogels. Chemical Engineering Science. 1991; 46(3):715–722.

Bunge AL. Release rates from topical formulations containing drugs in suspension. Journal of Controlled Release. 1998; 52(1):141–148. [PubMed: 9685944]

Coats AW, Redfern JP. Thermogravimetric analysis. A review. Analyst. 1963; 88(1053):906–924.

Colombo P. Swelling-controlled release in hydrogel matrices for oral route. Advanced Drug Delivery Reviews. 1993; 11(1–2):37–57.

Djuris J, Nikolakakis I, Ibric S, Djuric Z, Kachrimanis K. Preparation of carbamazepine–Soluplus® solid dispersions by hot-melt extrusion, and prediction of drug–polymer miscibility by thermodynamic model fitting. European Journal of Pharmaceutics and Biopharmaceutics. 2013; 84(1):228–237. [PubMed: 23333900]

Feng X, Vo A, Patil H, Tiwari RV, Alshetaili AS, Pimparade MB, Repka MA. The effects of polymer carrier, hot melt extrusion process and downstream processing parameters on the moisture sorption properties of amorphous solid dispersions. Journal of Pharmacy and Pharmacology. 2016; 68(5):692–704. [PubMed: 26589107]

Feng X, Ye X, Park JB, Lu W, Morott J, Beissner B, et al. Porter S. Evaluation of the recrystallization kinetics of hot-melt extruded polymeric solid dispersions using an improved Avrami equation. Drug Development and Industrial Pharmacy. 2015; 41(9):1479–1487. [PubMed: 25224341]

Gillespie, DT., Seitaridou, E. Simple Brownian diffusion: an introduction to the standard theoretical models. Oxford University Press; 2012.

Gross, BC., Erkal, JL., Lockwood, SY., Chen, C., Spence, DM. Evaluation of 3D printing and its potential impact on biotechnology and the chemical sciences. ACS Publications; 2014.

Higuchi T. Rate of release of medicaments from ointment bases containing drugs in suspension. Journal of Pharmaceutical Sciences. 1961; 50(10):874–875. [PubMed: 13907269]

Jain, KK. Drug Delivery Systems. 1st. Totowa: Springer; 2008.

Kalantzi L, Reppas C, Dressman JB, Amidon GL, Junginger HE, Midha KK, et al. Barends DM. Biowaiver monographs for immediate release solid oral dosage forms: Acetaminophen (paracetamol). Journal of Pharmaceutical Sciences. 2006; 95(1):4–14. [PubMed: 16307451]

Kojima H, Yoshihara K, Sawada T, Kondo H, Sako K. Extended release of a large amount of highly water-soluble diltiazem hydrochloride by utilizing counter polymer in polyethylene oxides (PEO)/polyethylene glycol (PEG) matrix tablets. European Journal of Pharmaceutics and Biopharmaceutics. 2008; 70(2):556–562. [PubMed: 18606223]

Korsmeyer RW, Gurny R, Doelker E, Buri P, Peppas NA. Mechanisms of solute release from porous hydrophilic polymers. International Journal of Pharmaceutics. 1983; 15(1):25–35.

Leong KW, Langer R. Polymeric controlled drug delivery. Advanced Drug Delivery Reviews. 1988; 1(3):199–233.

Liu X, Lu M, Guo Z, Huang L, Feng X, Wu C. Improving the chemical stability of amorphous solid dispersion with cocrystal technique by hot melt extrusion. Pharmaceutical Research. 2012; 29(3):806–817. [PubMed: 22009589]

Moulton SE, Wallace GG. 3-dimensional (3D) fabricated polymer based drug delivery systems. Journal of Controlled Release. 2014; 193:27–34. [PubMed: 25020039]

O'Connor TF, Lawrence XY, Lee SL. Emerging technology: A key enabler for modernizing pharmaceutical manufacturing and advancing product quality. International Journal of Pharmaceutics. 2016; 509(1):492–498. [PubMed: 27260134]

Paavola A, Kilpeläinen I, Yliruusi J, Rosenberg P. Controlled release injectable liposomal gel of ibuprofen for epidural analgesia. International Journal of Pharmaceutics. 2000; 199(1):85–93. [PubMed: 10794930]

Pani NR, Nath LK. Development of controlled release tablet by optimizing HPMC: Consideration of theoretical release and RSM. Carbohydrate Polymers. 2014; 104:238–245. https://doi.org/https://doi.org/10.1016/j.carbpol.2014.01.037. [PubMed: 24607183]

Paul DR. Elaborations on the Higuchi model for drug delivery. International Journal of Pharmaceutics. 2011; 418(1):13–17. [PubMed: 21034800]

Peppas NA, Narasimhan B. Mathematical models in drug delivery: How modeling has shaped the way we design new drug delivery systems. Journal of Controlled Release. 2014; 190:75–81. [PubMed: 24998939]

Peppas NA, Sahlin JJ. A simple equation for the description of solute release. III. Coupling of diffusion and relaxation. International Journal of Pharmaceutics. 1989; 57(2):169–172.

Repka MA, Langley N, DiNunzio J. Melt extrusion. Materials, Technology and Drug Product Design. 2013; 4:5.

Ritger PL, Peppas NA. A simple equation for description of solute release II. Fickian and anomalous release from swellable devices. Journal of Controlled Release. 1987; 5(1):37–42.

Santos HA, Salonen J, Bimbo LM, Lehto VP, Peltonen L, Hirvonen J. Mesoporous materials as controlled drug delivery formulations. Journal of Drug Delivery Science and Technology. 2011; 21(2):139–155.

Santus G, Baker RW. Osmotic drug delivery: a review of the patent literature. Journal of Controlled Release. 1995; 35(1):1–21.

Sarode AL, Malekar SA, Cote C, Worthen DR. Hydroxypropyl cellulose stabilizes amorphous solid dispersions of the poorly water soluble drug felodipine. Carbohydrate Polymers. 2014; 112:512–519. https://doi.org/https://doi.org/10.1016/j.carbpol.2014.06.039. [PubMed: 25129775]

Sarode AL, Obara S, Tanno FK, Sandhu H, Iyer R, Shah N. Stability assessment of hypromellose acetate succinate (HPMCAS) NF for application in hot melt extrusion (HME). Carbohydrate Polymers. 2014; 101:146–153. https://doi.org/https://doi.org/10.1016/j.carbpol.2013.09.017. [PubMed: 24299759]

Sarode AL, Sandhu H, Shah N, Malick W, Zia H. Hot melt extrusion (HME) for amorphous solid dispersions: predictive tools for processing and impact of drug–polymer interactions on supersaturation. European Journal of Pharmaceutical Sciences. 2013; 48(3):371–384. [PubMed: 23267847]

Serajuddin A. Solid dispersion of poorly water-soluble drugs: Early promises, subsequent problems, and recent breakthroughs. Journal of Pharmaceutical Sciences. 1999; 88(10):1058–1066. [PubMed: 10514356]

Siepmann J, Göpferich A. Mathematical modeling of bioerodible, polymeric drug delivery systems. Advanced Drug Delivery Reviews. 2001; 48(2):229–247. [PubMed: 11369084]

Siepmann J, Peppas NA. Modeling of drug release from delivery systems based on hydroxypropyl methylcellulose (HPMC). Advanced Drug Delivery Reviews. 2012; 64:163–174.

Siepmann J, Siepmann F. Modeling of diffusion controlled drug delivery. Journal of Controlled Release. 2012; 161(2):351–362. [PubMed: 22019555]

Stanković M, Frijlink HW, Hinrichs WLJ. Polymeric formulations for drug release prepared by hot melt extrusion: application and characterization. Drug Discovery Today. 2015; 20(7):812–823. [PubMed: 25660507]

Staples M, Daniel K, Cima MJ, Langer R. Application of micro-and nano-electromechanical devices to drug delivery. Pharmaceutical Research. 2006; 23(5):847–863. [PubMed: 16715375]

Vo AQ, Feng X, Morott JT, Pimparade MB, Tiwari RV, Zhang F, Repka MA. A novel floating controlled release drug delivery system prepared by hot-melt extrusion. European Journal of Pharmaceutics and Biopharmaceutics. 2016; 98:108–121. [PubMed: 26643801]

Ward C, Langdon SP, Mullen P, Harris AL, Harrison DJ, Supuran CT, Kunkler IH. New strategies for targeting the hypoxic tumour microenvironment in breast cancer. Cancer Treatment Reviews. 2013; 39(2):171–179. [PubMed: 23063837]

Weiniger CF, Golovanevski L, Domb AJ, Ickowicz D. Extended release formulations for local anaesthetic agents. Anaesthesia. 2012; 67(8):906–916. [PubMed: 22607613]

Willis L, Hayes D, Mansour HM. Therapeutic liposomal dry powder inhalation aerosols for targeted lung delivery. Lung. 2012; 190(3):251–262. [PubMed: 22274758]

Zhang J, Feng X, Patil H, Tiwari RV, Repka MA. Coupling 3D Printing with Hot-Melt Extrusion to Produce Controlled-Release Tablets. International Journal of Pharmaceutics. 2016

Highlights

- Novel and efficient manufacturing method by coupling of HME and 3D printing.
- Produce different structured tablets with designed drug released profiles.
- Tablets #3, 5, 6 and 9 can achieve zero order drug release.
- Structure and HPMC matrix contribute to the steady and constant drug release rates.
- Investigation of the correlation of the tablets structure and drug release profiles.

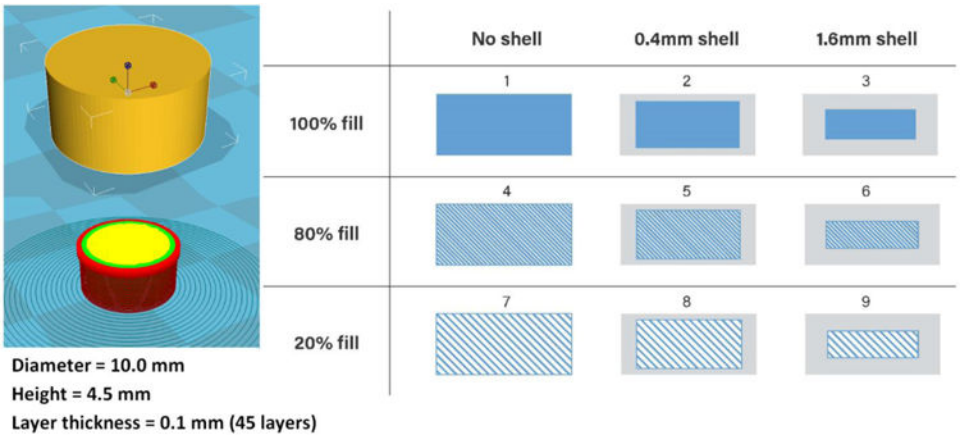

Figure 1.
3D tablet designs with varied outside shell thicknesses and inner core fill densities.

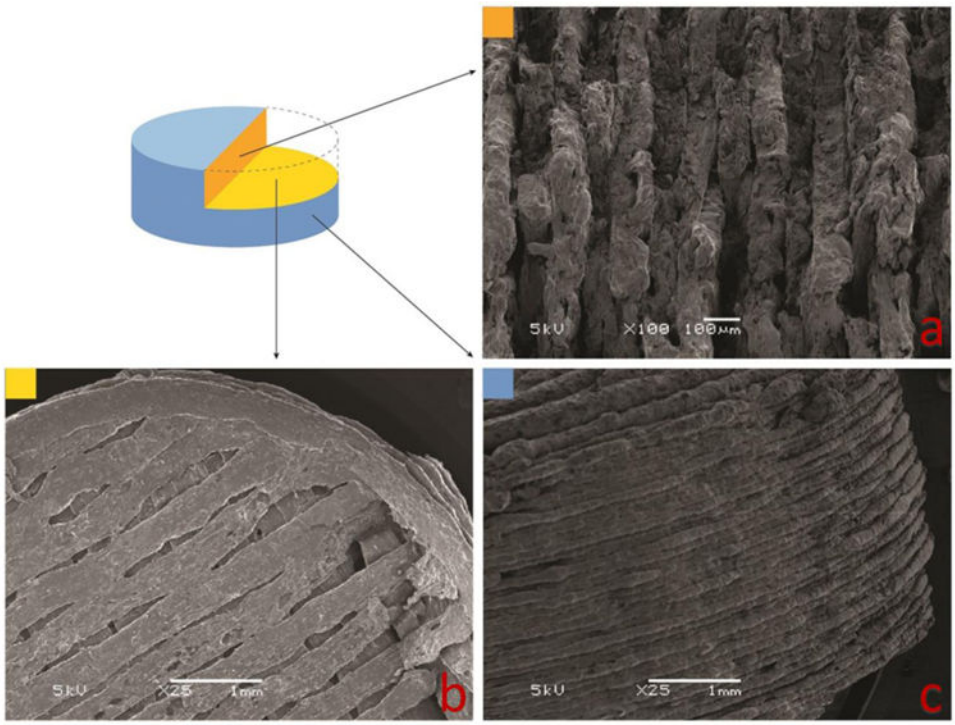

Figure 2.
3D structure of tablet #5, with a 0.4 mm shell and 80% inner fill.

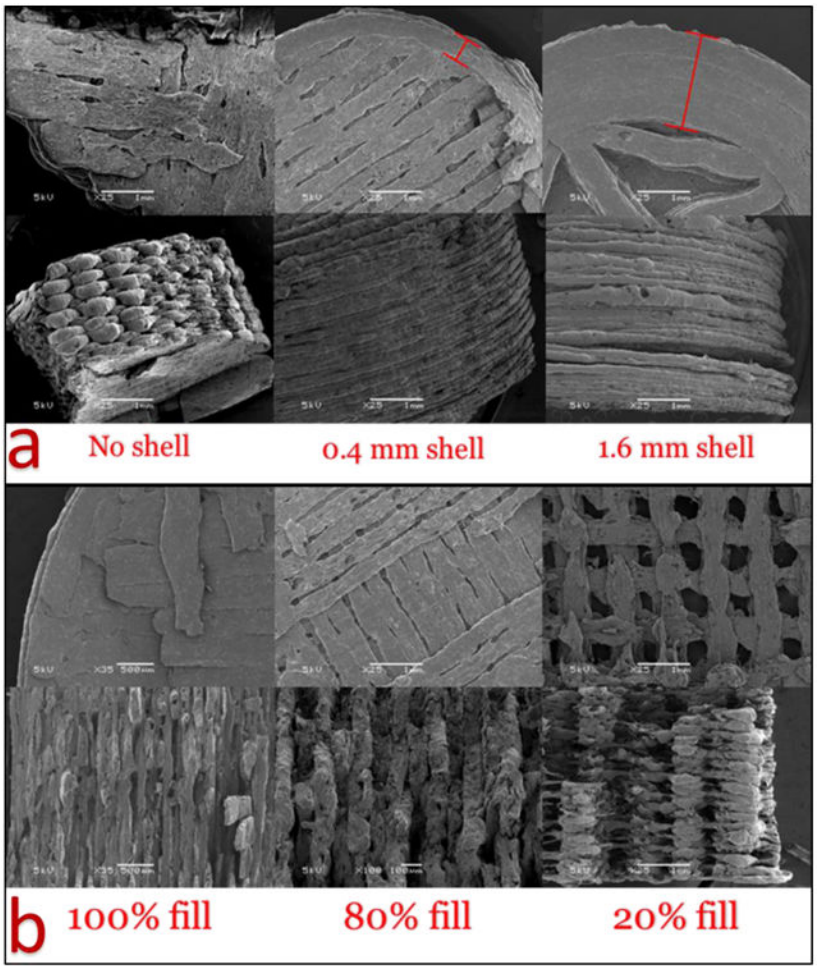

Figure 3.

a) 3D structures of tablets printed with no shell or with shells of 0.4 and 1.6 mm thickness; b) Tablets with 100, 80, and 20% inner core fill density.

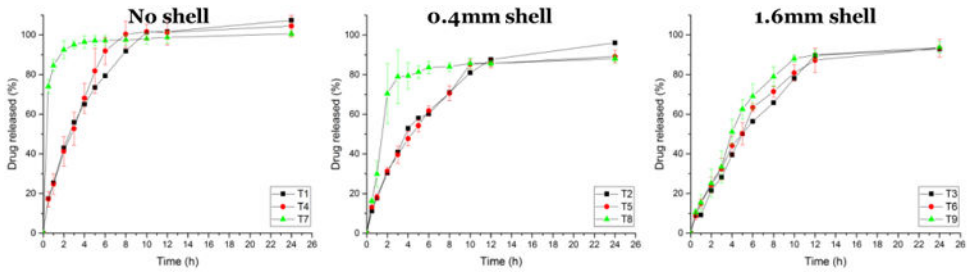

Figure 4.

In vitro drug release profiles of tablets (T) with no shells and with shells of 0.4 and 1.6 mm thickness.

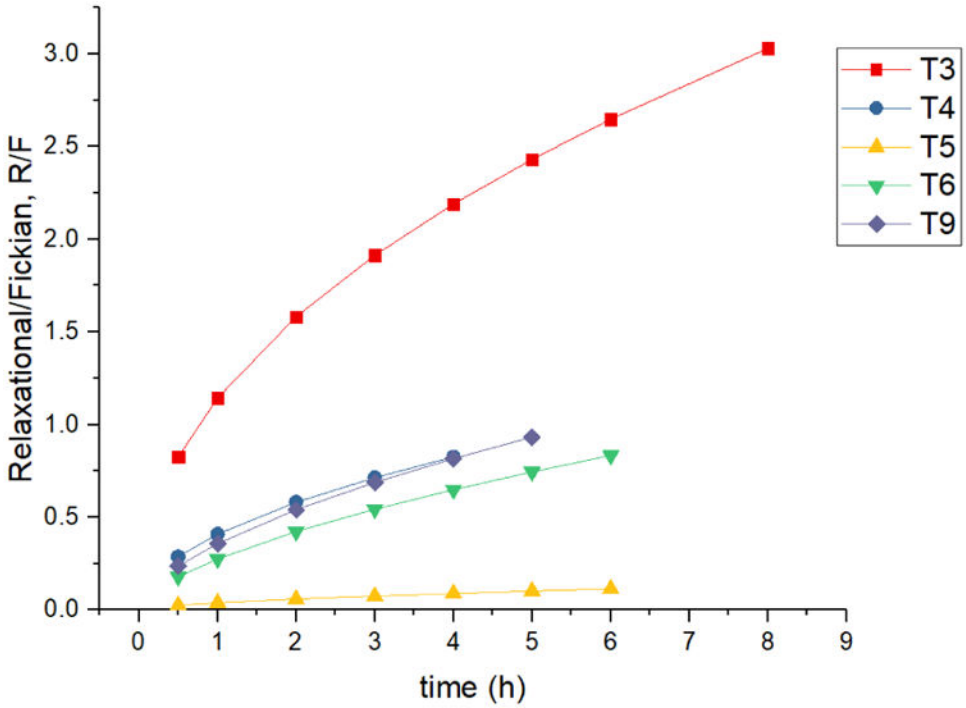

Figure 5.
Swelling contribution, R to diffusion contribution, F ratio from tablets #3, 4, 5, 6, and 9.

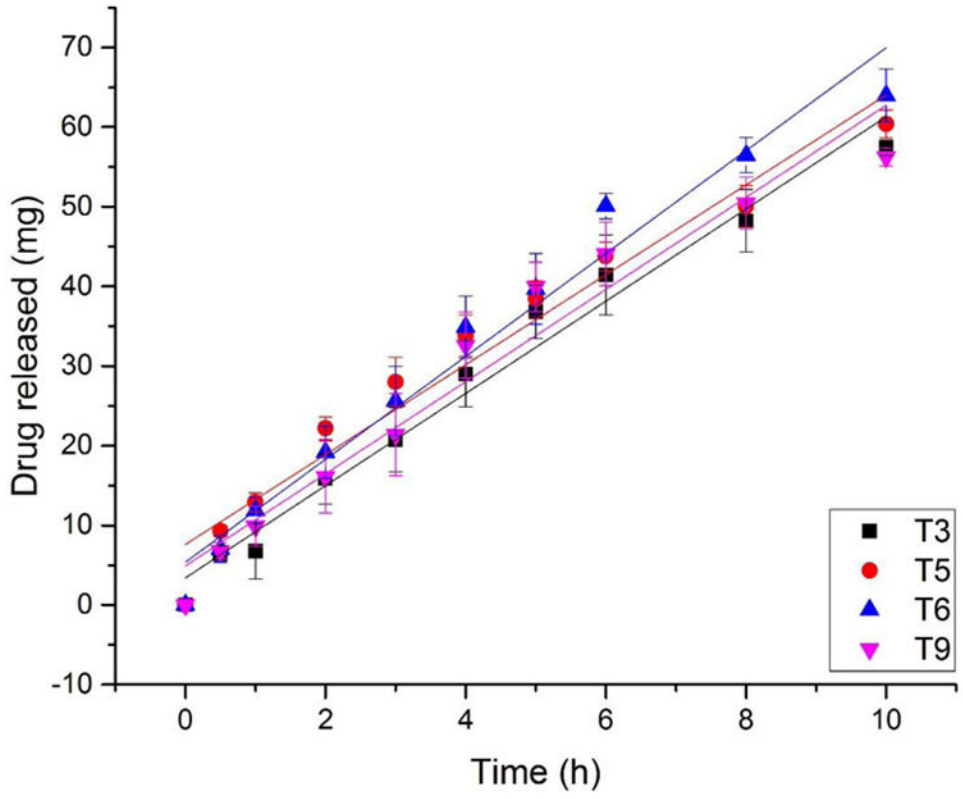

Figure 6.
Linear fitting of drug release from tablets #3, 5, 6, and 9 over 10 h.

Table 1

Geometric characteristics of the 3D printed tablets.

	Shell (mm)	Fill %	Diameter (mm)	Thickness (mm)	Weight (mg)	Density (mg/mm^3)	Porosity (%)	Hardness (kp)
T1	0	100	11.22±0.07	4.46±0.05	435.45±15.21	0.988	0	OV*
T2	0.4	100	10.51±0.24	4.22±0.21	377.91±24.73	1.030	0	OV*
T3	1.6	100	10.33±0.28	4.40±0.22	366.93±26.12	0.992	0	OV*
T4	0	80	10.91±0.30	4.29±0.19	352.04±24.94	0.877	20	OV*
T5	0.4	80	10.47±0.16	4.42±0.05	354.19±16.92	0.931	13.97	32.8±5.6
T6	1.6	80	10.36±0.19	4.47±0.02	395.58±18.72	1.050	2.71	32.2±5.3
T7	0	20	10.28±0.18	4.35±0.16	176.51±12.65	0.489	80	2.7±1.4
T8	0.4	20	10.21±0.16	4.48±0.05	197.19±11.62	0.538	55.82	5.3±4.2
T9	1.6	20	10.39±0.25	4.41±0.22	319.34±10.46	0.854	10.51	23.8±6.5

*OV= over detection limit

Table 2

In vitro dissolution parameters of the 3D printed tablets.

	Ritger-Peppas model		Linear model		Peppas-Sahlin model			
	Exponent, n	R^2	Slope, k	R^2	k_1	k_2	m	R^2
T1	0.59	0.9872	7.14	0.8881	0.29014	-0.0277	0.8509	0.9975
T2	0.69	0.9924	5.28	0.9254	0.20396	-0.0145	0.8348	0.9956
T3	0.78	0.9808	5.46	0.9790	0.06398	0.0732	0.4685	0.9861
T4	0.71	0.9968	6.02	0.8472	0.18201	0.0746	0.5061	0.9949
T5	0.64	0.9973	4.97	0.9399	0.18909	0.0074	0.6001	0.9968
T6	0.82	0.9968	5.82	0.9585	0.11352	0.0314	0.6168	0.9979
T7	0.10	0.8971	1.41	0.2995	-	-	-	-
T8	0.67	0.9801	2.36	0.5606	-	-	-	-
T9	0.79	0.9900	5.00	0.9271	0.12184	0.0437	0.5939	0.9869

*T7, T8 parameters were not calculated because their released rate too fast (over 60% in 2 h).